Multimedia Tools and Applications (2024) 83:14085–14109
https://doi.org/10.1007/s11042-023-16274-0

Face recognition for human identification through integration of complex domain unsupervised and supervised frameworks

Swati Srivastava[1] · **Himanshu Sharma**[1]

Received: 19 March 2022 / Revised: 22 May 2023 / Accepted: 4 July 2023 /
Published online: 12 July 2023

Abstract
Human identification can be performed through various available biometric traits such as the face, iris, fingerprint, ECG, gait, and ear. Among them, face is one of the most popular and widely used biometrics. In the security domain, early warnings and the trace of suspects can be accomplished using face recognition. The contemplated augmentation projected an intelligent computational model for human recognition which is an ingenious melding of unsupervised outline and complex domain neurocomputing. The unsupervised framework of our proposal constitutes evolutionary fuzzy computations in complex domain. The supervised schema capitalizes on a complex domain neural network with higher-order neurons and resilient propagation algorithm. Trainable multiple stages are populated in this proposal for the estimation of recognition and classification. This proposal offers an intelligent performance on recognition and classification tasks. Comprehensive experimental analysis on the datasets of AR face, PubFig83, and Indian face evidenced the enhanced precision of the proposed model. Our model achieves an impressive accuracy range of 97% to 99% across all datasets. These results clearly demonstrate the superior performance of our approach, showcasing the dominance of the combined unsupervised and supervised frameworks over other state-of-the-art methods.

Keywords Supervised · Unsupervised · Face recognition · Human identification · Complex domain · Neural network · Fuzzy clustering · Evolutionary computation

1 Introduction

Advances in the direction of human identification [58] through face have been continuously growing. Although it is one of the old biometric traits, still it needs imperative advancements. In the last two decades, it is highly investigated biometric [58]. The application

✉ Himanshu Sharma
himanshu.sharma@gla.ac.in

Swati Srivastava
swati.srivastava@gla.ac.in

[1] Department of Computer Engineering and Applications, GLA University, Mathura, India

layout of human identification includes attendance access control, security, and finance, accessing control, smart cards, and surveillance. A comprehensive variety of models exist including single technique based as well as multiple technique based to estimate recognition and classification. This inspired us to implement a fast recognition system based on the unification of unsupervised and supervised outlines which can be considered as an innovative approach in the field of face biometric systems. In this proposal, the notion is to take assistance from the virtues of both unsupervised and supervised learning. In this paper, an approach for face recognition is proposed using evolutionary fuzzy computations with complex neurocomputing. The projected model is robust to deal with images captured in an unconstrained environment. The proposed system offers enhanced recognition and classification inferences by providing speedy convergence, reduced complexity, and better precision. The unsupervised module is fabricated with fuzzy computations supplemented with the evolutionary approach. Complex neurocomputing module employs the nonlinear neuron model and efficient learning which presents improved learning competence of the network. This boosted the performance of the neurocomputing module in turn strengthen the dominance of the overall model. In this proposal, multivariate statistical techniques provide low dimensional data which is input to the unsupervised framework. The complex evolutionary fuzzy computation is incorporated by the complex Neurocomputing in an innovative manner such that the outcome of the unsupervised outline establishes the structure of the neural classifier. The presented learning machine offered enhanced precision with low complexity and lesser learning cycles even in unconstrained situations. The proposed model has been intensely examined over AR face, PubFig83, and Indian face datasets.

The main contributions of the proposed work are:

- Feature representation using unsupervised linear mapping and supervised linear dimensionality reduction technique.
- Design a model based on the consolidation of complex unsupervised and complex supervised frameworks with higher-order neuron and resilient propagation learning.
- Extensive experimental analysis has been conducted that illustrated the superior position of the proposed recognizer among previous models on AR face, PubFig83, and Indian face datasets.

Figure 1 depicts the fundamental building blocks of the face recognition system. The current necessity of security scenarios [34, 41, 67] still insists to design a robust system to deal with varied distinctions in face expression, orientation, postures, and brightness as shown in Fig. 2. Therefore, to develop an efficient and fast recognizer is the need of an hour.

The rest of this paper is organized as: An overview of earlier works towards hybrid models, classifiers, neurons, learning algorithms, and domain of implementation is presented in Section 2. Section 3 introduces the projected model. Experimental results are reported in Section 4 for different combinations of hidden neurons and learning algorithms. It also presents the ablation study along with the comparison with state-of-the-art which presented the superiority of our model. Finally, the work is concluded in Section 5 with some future directions.

Fig. 1 Basic Framework of the face recognition system

Fig. 2 Sample variations in facial expressions, backgrounds, illumination, and postures

2 Related works

2.1 Hybrid models

For face recognition systems, single technique-based methods [3, 66] work well for constrained settings. However, they are not efficient for the natural environment. It has been observed from literature that the systems based on multiple techniques work in a more efficient manner than unaccompanied technique-based systems. For example, Mantoro et al. [48] used Haar Cascades and Eigenfaces to recognize multiple faces with 91.67% accuracy. Shamrat et al. [38] used Principal Component Analysis (PCA) to analyze the features and speed up the robust features (SURF) technique for identification and claimed an almost similar recognition rate as in existing methods on the ORL dataset. The limited learning capabilities of PCA need to be addressed. Abuzneid et al. [1] presented an enhanced approach for face recognition based on the unification of multiple techniques like Local binary patterns histogram (LBPH) descriptor, multi-K nearest neighbor (KNN), and back-propagation where they achieved competitive performance on benchmark datasets. Roh et al. [55] proposed a face recognition method based on fuzzy transform and radial basis function neural networks (RBFNN) that analyze the distribution of data over the input spaces where they fail to optimize the fuzzy partitions. Gupta [31] used Discrete Cosine Transform (DCT) to reduce information redundancy which constructs a feature vector and used Neural Network (NN) for classification. Lukas et al. [47] proposed a method for face recognition where Discrete Wavelet Transforms (DWT) and Discrete Cosine Transform (DCT) are used for feature extraction and Radial Basis Function (RBF) is used for classification and achieved an 82% recognition rate. Rejeesh [54] proposed a recognition system where Adaptive Genetic Algorithm (AGA) is used to optimize the parameters. They used an Adaptive neuro-fuzzy inference system (ANFIS) along with Artificial Bee Colony Algorithm (ABC) for classification where training parameters are optimized for enhanced performance. All above mentioned syntheses aimed to provide better recognition. The system can be hybrid either at the technique level or data level such as a fusion of multi-modalities [50]. In continuation with hybrid systems, we proposed a method based on the unification of unsupervised and supervised frameworks.

2.2 Classifiers

Researchers employed various classifiers in different classification models which include Sigmoid regression, naive Bayes, Support Vector Machine (SVM), decision trees, and

NN [15, 44, 57, 59, 60]. Among them, the NN classifier is substantially noticeable for investigators due to its endowed upshots and extensive pertinency. In the NN classifier, we can enhance the performance at three levels: at the neuron level, at the learning algorithm, and domain of implementation. Here we have worked on all three levels. A neural network with conventional neural structures works well with a large number of conventional neurons to achieve the desired consequences. To reduce this requirement, we can move from traditional neurons to higher-order neurons.

2.3 Neurons in neural network

For high dimensional input data, it cannot be predicted how long the neural network with conventional neurons will take for the learning process. Also, it requires a large number of hidden neurons and output neurons for convergence at a satisfactory level. For improved consequences and speedy convergence of conventional NNs, wide-ranging attempts took place to evolute higher-order neurons. The attempts in this direction include pi-sigma [16, 17], quadratic neurons [21–23, 70] and other higher order neurons [64, 65]. The advancement of higher-order neurons is rising continuously. Its employment boosted the efficiency of many classification models. Higher-order neurons offered ingenious performance over conventional neurons [21, 70]. Although, the computational complexity increases with the engagement of higher order neurons the need for relatively very few neurons for the purpose indemnifies the aforesaid mentioned intricacy along with boosted performance. Accordingly, we employed higher-order neurons in our proposal.

2.4 Learning algorithms

The conventional NN employs a backpropagation (BP) learning algorithm [29, 33] which is less précised with unrushed convergence. With the outspread intention of researchers in the direction of performance progression, the resilient propagation (RPROP) learning algorithm came into portrait as an enhancement upon the backpropagation learning. RPROP [14, 36] offers effectually speedy convergence and better precision compared to the BP algorithm. The indicated progression galvanized us to employ an RPROP learning algorithm with a higher-order neuron structure which would impart accelerated convergence with enhanced precision as compared to RPROP learning with conventional neurons. Performance can be further improved by implementing the network in complex domain.

2.5 Domain of Implementation

The real-valued NN has leading restrictions of lethargic convergence and the predicament of getting stuck into local minima. The real-valued classifier was dragged to the complex domain [51] for the sole purpose of enhanced performance. They offer to regulate robust nonlinear input-output mapping and superior estimation aptitude over conventional neural networks. A complex domain network better approximates the phase information as it is embedded in complex number. Complex domain implementation clipped the standstill probability and provide speedy convergence which has been proclaimed in [7, 39, 51]. The supremacy of complex-valued networks is contemplated in [28, 45, 64, 65, 68]. So, a

computational illustrative along with higher order neurons and fast learning algorithm in complex domain can give boosted performance. The complex-valued network overcomes the issues of a real-valued network by lessening the local minima predicament with accelerated convergence.

2.6 Motivation

To overcome the limitations of existing face recognition methods and to achieve enhanced performance is the motivation of current work. We proposed a multiple technique-based framework that focuses on addressing the limitations of existing methods. **First,** for dimensionality reduction, eigenface-based algorithms are used in existing methods which have the limitation of weak learning capabilities. To overcome this limitation, we have used Fisherface which works better with large datasets having multiple classes where class separability is important while reducing dimensionality. **Second,** for unsupervised learning, we considered fuzzy clustering as it is observed in studies that fuzzy c-means clustering performs comparatively better than the k-means algorithm. As in fuzzy clustering, a class may belong to more than one cluster, unlike k-means where the data point must exclusively belong to one cluster. The limitation of fuzzy clustering is its stochastic nature. To handle this limitation, we have used evolutionary computation that can self-adapt to the search for optimum solutions. **Third,** for supervised learning, it is evident from studies that k- nearest neighbors (KNN), support vector machine (SVM), Random Forest, and logistic regression have limited classification accuracy for large training data. To enhance the performance, we elected neurocomputing for our proposal as large training data neural networks (NN) achieve sufficient accuracy. NN performs better than a support vector machine (SVM) when the number of features is higher than the number of training samples. These dominances of NN make it the most suitable classifier for our proposal. Thus, in our proposal, eigenface with fisherface archetype is used to extract the desired features from input images. Fuzzy c-means clustering along with evolutionary computation constitutes the unsupervised module to get the optimized fuzzy distribution. Lastly, neurocomputing is used in supervised module for classification.

3 Unsupervised-supervised integrated framework (USIF)

The proposed model is based on the novel assimilation of the complex-valued unsupervised framework with complex-valued Neurocomputing. Our model accomplished the task of recognition and classification by employing eigenface, fisherface, complex fuzzy clustering with evolutionary computation, and a complex-valued neural network. In studies, it is demonstrated that fuzzy clustering performs comparatively better than the k-means algorithm. For labeled data in the proposed model, each class is assigned membership to one or more clusters. Consequently, a class may belong to more than one cluster, unlike k-means where the data point must exclusively belong to one cluster. Due to the stochastic nature of fuzzy clustering, the evolutionary scheme is taken into consideration. Evolutionary computation can self-adapt to the search for optimum solutions. An evolutionary fuzzy approach is a learning estimation that harmonizes fuzzy logic with evolutionary computation. The approach aims to syndicate

the optimization and learning aptitudes of evolutionary and fuzzy computations. Thus, the unsupervised module of the presented model employs fuzzy logic further complemented with evolutionary computation to encounter the optimal unsupervised distribution of input classes. This optimal solution is the result of the unsupervised outline of the proposed model. This upshot is the pertinent output used by the neural classifier. This proposal elected neurocomputing for the classification module as it outperforms classical machine learning (ML) algorithms. From studies, it is evidenced that for large training data, neural networks (NN) achieve sufficient accuracy compared to the k- nearest neighbors (KNN) algorithm and Random Forest. Neural network models are more flexible as compared to Sigmoid regression. NN performs better than support vector machine (SVM) when the training features are higher in number than the training samples. These dominances of NN make it the most suitable classifier for our proposal. Thus, the virtue of each conception streamed in the proposed model devised the learning machine with speedy convergence, and improved error optimization with intensified recognition correctness. Figure 3 depicts the proposed Unsupervised-Supervised Integrated Framework (USIF). An uninvestigated amalgamation of complex unsupervised and complex supervised frameworks leads to an innovative model which systematically demonstrated its dominance over an extensive range of methods.

3.1 Eigenface fisherface (EF) based feature representation

The anticipated computation of any computer vision system begins with dimensionality reduction. A lower dimensional subspace apprehends the spirit of corresponding high dimensional data. Reduced input variables eventuate in a simpler predictive model that may perform better when making predictions on new data. Hunt out an appropriate representation for multivariate data [20, 32, 63] is a vital problem in

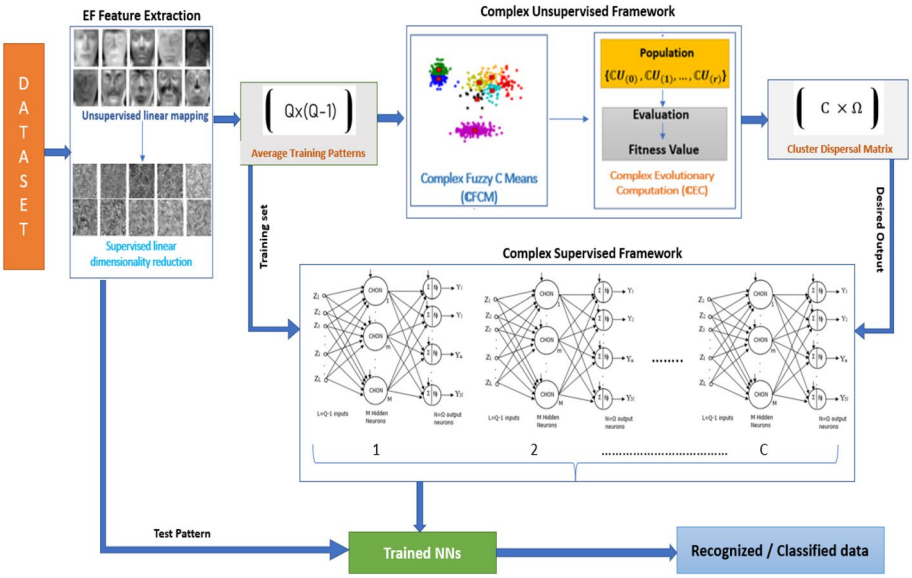

Fig. 3 Proposed Integration of Unsupervised and Supervised Frameworks

computer vision. High-dimensional data is inefficient for any computation as it may be highly correlated and challenging to represent. The computation of the proposed model initiates with unsupervised linear mapping based on eigenvectors. In the computer vision problem of human face recognition, an eigenface [18, 46] refers to the set of eigenvectors. The eigenvector corresponding to the highest eigenvalue preserves the maximum extent of variance of the original data. Each succeeding eigenvector has the next highest variance which is orthogonal to the preceding eigenvectors. The consequential vectors represent the uncorrelated data. Few uncorrelated features are extracted that contain maximum information sufficient to envision data in low dimensional space. These uncorrelated features are then fed into the fisherface process [6, 26, 35, 69] which delineates a hefty number of features onto a reduced dimensional space. Linear supervised approach for dimensionality reduction projects huge statistics of features onto a low-dimensional space with erect class separability. When the goal is classification rather than representation, we go for minimizing within-class differences and maximizing between-class distances. Thus, the image dataset is converted into fisher face vectors. This yields a reduction in computational cost although retaining the spirit of original data for expressive investigation. This low-dimensional data is then used in subsequent modules of the proposed model. Algorithm 1, to excavate the relevant features of the image dataset, is presented below.

3.2 Complex valued unsupervised framework

This module initiates with complex fuzzy-c-means ($\mathbb{C}$FCM) clustering to which the entire dataset is provided as input. As shown in Fig. 3, complex fuzzy clustering is applied to the average training patterns of input data to conquer the fuzzy dispersal of input classes. This fuzzy division revealed the allocation of clusters to input classes. The optimized cluster cannot be attained by solitary fuzzy clustering due to its stochastic behavior. Consequently, it results in, unlike partitions in different runs. The different populations establish an optimization problem. To acquire an optimized partition among the number of attained divergent fuzzy distributions, evolutionary computation is taken into consideration. To approximate the resolution of the indicated optimization problem, the fitness [43] of each discrete population is estimated. The population with the uppermost fitness value is preferred among all populations. This population will act like the initial population for the subsequent generation. This process repeats for several generations until the difference between two successive distributions is within or equal to the specified threshold. Hence, the fuzzy distributions attained from the fuzzy algorithm are administered based on the survival of the fittest to catch the optimized division. This optimized distribution is the initial distribution for subsequent generation. The process lasts till the difference in distributions for the two generations is less or equal to the defined threshold. The distribution for the last generation is the optimal one. As discussed in Algorithm 2 for unsupervised module, this fuzzy optimal distribution is converted to crisp distribution. This is used as the target output for the complex supervised module of the proposed model. In an innovative unification of unsupervised and supervised frameworks, the optimal distribution decides the assembly of the complex neural classifier. Before initiating the computations for the unsupervised outline, average training patterns of classes are computed which is a more compact representation.

Algorithm 1: EF Feature Representation

Input: *Let an* $a \times a$ *image is expressed as a linear vector* I_i *of size* a^2 *and P be the total samples in the dataset represented as a matrix of dimension* $(P \times a^2)$ *as* $A = \{I_1, I_2, \ldots \ldots, I_P\}$

1. Calculate the mean of matrix A, $A_{avg} = \frac{1}{P}\sum_{k=1}^{P} I_k$

2. Estimate adjusted data matrix $D = A - A_{avg}$

3. Find covariance matrix $\chi = D \times D^T$ *(size:* $a^2 \times a^2$*)*

4. Calculate eigenvalues and eigenvectors to reduce the dimensions to P and to diminish the dimensions additionally, k eigenvectors are selected corresponding to k prominent eigenvalues as $F = \{F_1, F_2, \ldots \ldots, F_k\}$

5. Eigenface-based features G are obtained by projecting D onto eigenface space F as: $G = F^T \times D$

6. The optimal subspace S is figured as: $S = \left|\frac{A^T \gamma_{bet} A}{A^T \gamma_{within} A}\right|$, *where*

$$\gamma_{bet} = \sum_{i=1}^{Q} B \times \left[\frac{1}{B}\left(\sum_{j=1}^{B} G_j^i\right) - \frac{1}{P}\sum_{j=1}^{P} G_j\right] \times \left[\frac{1}{B}\left(\sum_{j=1}^{B} G_j^i\right) - \frac{1}{P}\sum_{j=1}^{P} G_j\right]^T$$

and

$$\gamma_{within} = \sum_{i=1}^{Q} \sum_{j=1}^{B} \left[G_j - \frac{1}{B}(G_j^i)\right] \times \left[G_j - \frac{1}{B}(G_j^i)\right]^T$$

with the assumption that B be the number of images in each class.

7. The unfolding of above computation is like denominating the eigenvectors matching to top $Q-1$ *eigenvalues* β_i *by solving* $\gamma_{bet} G_i = \beta_i \gamma_{within} G_i$, *where* $i = 1,2, \ldots, Q-1$ *and* Q *is the number of classes.*

8. Discriminant eigenface features H is attained by projecting eigenfaces G on optimal subspace S as $H = S^T \times G$ *(size:*$(P \times (Q-1))$ *).*

Output: *Dataset with diminished dimensions as matrix H of size (P×(Q-1)), where Q is the number of classes.*

Algorithm 2: Complex Unsupervised Framework

Input: *Average pattern matrix* $\mathbb{C}X$.

$\mathbb{C}$***FCM (Complex Fuzzy-c-means)***

1. Fix the value of C (number of clusters), and initialize the complex distribution $\mathbb{C}U$ *of dimension* $C \times Q$. *The primary population* $\mathbb{C}U_{(0)} = [\mathrm{R}\alpha_{ij} + i\,(\xi\alpha_{ij})]$ *is arbitrarily initialized as* $\alpha_{ij} \in [0,1]$, *where* $1 \le i \le C$ *and* $1 \le j \le Q$.

2. Revise $\mathbb{C}U_{(0)}$ *as* $\mathbb{C}\alpha_{ij} = \left(\frac{\mathrm{R}\delta_{ij}^{\frac{-2}{\jmath-1}}}{\sum_{k=1}^{C} \mathrm{R}\delta_{kj}} + i \times \frac{\xi\delta_{ij}^{\frac{-2}{\jmath-1}}}{\sum_{k=1}^{C} \xi\delta_{kj}} \right)$ *where* $\mathbb{C}\,\delta_{ij} = \left(\sum_{p=1}^{Q-1} \left\| \mathbb{C}\,\bar{x}_{jp} - \mathbb{C}c_{ip} \right\|^{\aleph} \right)^{\aleph-1}$ *is the distance of* j^{th} *class from* i^{th} *cluster,* $\aleph$ *and* $\jmath$ *are the hyperparameters called as generalization parameter and fuzzifier respectively.*

3. Calculate cluster centers (centroid) as $\mathbb{C}c_i = \left(\frac{\sum_{j=1}^{Q} \mathrm{R}\alpha_{ij}{}^{\jmath} \mathrm{R}\overline{x_j}}{\sum_{j=1}^{Q} \mathrm{R}\alpha_{ij}{}^{\jmath}} + i \times \frac{\sum_{j=1}^{Q} \xi\alpha_{ij}{}^{\jmath} \xi\overline{x_j}}{\sum_{j=1}^{Q} \xi\alpha_{ij}{}^{\jmath}} \right)$

4. Update objective function as

$$\mathbb{C}J = \sum_{i=1}^{C} \sum_{j=1}^{Q} \mathrm{R}\alpha_{ij}{}^{\jmath} \mathrm{R}\,\delta_{ij} + i \times \sum_{i=1}^{C} \sum_{j=1}^{Q} \xi\alpha_{ij}{}^{\jmath}\, \xi\,\delta_{ij}$$

5. Repeat the above steps until convergence i.e. if $\|\mathbb{C}J(\alpha, c)^{t+1} - \mathbb{C}J(\alpha, c)^{t}\| < \vartheta$ *for t > 1, where t is iteration and* ϑ *is the threshold.*

6. The above steps result in a fuzzy partition $\mathbb{C}U_{(1)}$.

$\mathbb{C}$***EC (Complex Evolutionary Computation)***

7. Calculate the fitness value for r attained fuzzy distributions $\{\mathbb{C}U_{(0)}, \mathbb{C}U_{(1)}, \ldots, \mathbb{C}U_{(r)}\}$ *by exploiting fitness function* $\mathbb{C}\mathcal{F} = \left(\frac{\mathrm{R}Q \times \mathrm{R}d_{min}}{\sum_{i=1}^{C} \sum_{j=1}^{Q} \mathrm{R}\alpha_{ij}{}^{\jmath} \mathrm{R}d} + i \times \frac{\xi Q \times \xi d_{min}}{\sum_{i=1}^{C} \sum_{j=1}^{Q} \xi\alpha_{ij}{}^{\jmath} \xi d} \right)$

where $\mathbb{C}d = \sum_{i=1}^{C} \sum_{j=1}^{Q} \left\| \mathrm{R}\,\overline{x_j} - \mathrm{R}c_i \right\|^2 + i \times \sum_{i=1}^{C} \sum_{j=1}^{Q} \left\| \xi\,\overline{x_j} - \xi c_i \right\|^2$

8. The partition with the maximum fitness value is picked.

9. This partition is considered as the primary population for the next generation.

10. Repeat for g generations until $\left\| \mathbb{C}U^{(g+1)} - \mathbb{C}U^{(g)} \right\| \le \rho$ *(for g>1)*

11. The partition obtained for the last generation is mentioned as optimal distribution $\mathbb{C}U^{(opt)}$.

12. In $\mathbb{C}U^{(opt)}$, *organize the classes in descending order of their membership degree.*

13. Select top Ω *elements to ensure the even-sized clusters.*

14. From $\mathbb{C}U^{(opt)}$ *with* Ω *number of columns, consider the real part* $\mathbb{R}U^{(opt)}$ *for next step.*

15. The fuzzy membership real values are then transformed to equivalent class to get the crisp values ensuing in $CDM \leftarrow \mathbb{R}U^{(opt)}(1{:}C, 1{:}\Omega)$ *where* $\Omega < Q$.

Output: $CDM \leftarrow \mathbb{R}U^{(opt)}(1{:}C, 1{:}\Omega)$ *% Cluster dispersal matrix*

The mean pattern of q (q < B) training data for j^{th} class is expressed as: $\overline{x_j} = \frac{1}{q}\left(\sum_{k=1}^{q} x_{kj}\right)$, where $1 \leq j \leq Q$. The obtained matrix is X of size $(Q \times (Q-1))$. Transform X into complex X denoted as $\mathbb{C}$X by using Hilbert Transform [40]. Thus, the complex average training patterns will be used as input to the complex unsupervised framework of the proposed model. In this work, $\mathbb{C}$ denotes a complex number and $\mathbb{R}$ denotes a real number. Also, $\mathcal{R}$ and ξ denote the real and imaginary parts of a complex number respectively.

3.3 Complex valued supervised framework

Complex neurocomputing is one of the segments channelized in the architecture of the proposed model. Algorithm 3 presented the steps involved in a supervised framework. In this work, the conventional summation aggregation neuron is denoted as SAN. Training of the network is accomplished according to the outcome of the unsupervised outline. Weights and biases modification for error optimization engaged the complex resilient propagation ($\mathbb{C}$RPROP) algorithm. The effectiveness of $\mathbb{C}$RPROP is further boosted with higher-order neurons [62] based on summation, radial basis, and their product. The classifier with complex higher-order neurons ($\mathbb{C}$HON) and $\mathbb{C}$RPROP lead to lessened computational cost and speedy convergence with higher accuracy. The exploitation of $\mathbb{C}$HON enormously diminishes the complexity of the proposed learning machine as very few higher-order neurons are adequate for efficient recognition and classification compared to conventional neurons. The $\mathbb{C}$RPROP algorithm is used for error optimization which offers enhanced performance over both real and complex backpropagation learning.

Algorithm 3: Complex Supervised Framework

Input: *Training set: Average Training Patterns* $\mathbb{C}$X*; Test set: low dimensional data H; Cluster dispersal matrix* $CDM \leftarrow \mathbb{R}U^{(opt)}(1{:}C, 1{:}\Omega)$ *as pertinent output for the network.*

Training: The networks are trained on $\mathbb{C}$X*, for which known I/O alignment is available as* CDM.

Testing: Compute the output as matrix Ł of size $C \times \Omega$ *for* k^{th} *test pattern.*

1. $[O_{ki}, \tau_i] \leftarrow \text{Max}\,(Ł)$
2. $[\square, \tau'] \leftarrow \text{Max}_{i=1}^{C}(O_{ki})$
3. $R \leftarrow \text{CDM}\,(\square, \tau')$
4. *The integrity of* $[(mod(k,Q) > 0 \;\&\&\; (R = mod(k,Q))]$ *or* $[(mod(k,Q) = 0 \;\&\&\; (R = Q)]$ *validate the accuracy of* k^{th} *test pattern.*

Output: *Test pattern recognized and classified.*

The superiority of $\mathbb{C}$HON accompanied by the fast-learning algorithm $\mathbb{C}$RPROP holds a potential that enables the proposed method to provide an improved recognition rate with the lessened number of training cycles and speedy convergence. For computational congruity, the complex-valued input is more appropriate to be fed into the complex-valued neural network. Thus, the complex average training patterns $\mathbb{C}$X will be used as input to the complex supervised framework of the proposed model. The trained model is then evaluated on the test patterns for classification and recognition. The trade-off between computational cost and number of neurons balances the computational cost. Hence, the use of higher-order neurons makes the system efficient which offers enhanced classification with fast convergence.

4 Experimental results and analysis

4.1 Datasets

We have evaluated our model on three widely accessible datasets:

AR face dataset We have used the AR face dataset [49] to evaluate our model. It incorporates approx. 4000 images of 126 subjects. It contains images of 70 males and 56 females. Image acquisition took place in two sessions parted by a couple of weeks. 13 images per subject were captured in each session. One for each: Neutral expression, smile, annoyance, yell, left light, right light, both lights, wearing glasses, wearing glasses with left light, wearing glasses with the right light, wearing a scarf, wearing a scarf with left light, wearing a scarf with the right light. Thus, the images of a subject follow variations in brightness conditions, expressions, and occlusions. We used 80% and 20% of images for training and testing respectively. Database images of one subject are shown in Fig. 4.

PubFig83 Dataset The second dataset under consideration to approximate our model is Pubfig83 [52]. This is a dataset of public face images scrapped from the web. It consists of nearly 60 K images of 200 people. Most of them are popular celebrities. This is a bulky dataset where images are acquired in wholly wild conditions without the cooperation of subjects. Due to the unconditional environment, images possess large divergence in posture, radiance, advent, scene, sensor eminence, imaging settings, and other parameters. Initially, the PubFig database was introduced containing two hundred subjects with an inconstant number of images. Later a subgroup of the original PubFig dataset entitled PubFig83 was familiarized. It includes 8 K plus images of 83 subjects with unhindered diversities of appearance, stance, occlusion, lighting, and resolution. We used a PubFig83 version that was offered by [11]. 80% and 20% of images are selected for training and testing respectively. Figure 5 shows some sample images from PubFig83 faces.

Indian Face Dataset We have also used the Indian face dataset [37] (IITK dataset) to estimate our model. It contains 11 images each for 40 distinct subjects including both male and female. Eleven images follow different facial orientations such as front, left, right, up, up towards left, up towards the right, and down, and different facial emotions such as: impartial, happy, chuckle, and unhappy. The database with such wide deviations is a worthy facet to assess any model. The images are sized 640×480 with 256 grey levels. A few sample images are shown in Fig. 6. 80% of the database images are used in training while another 20% of images are used for testing.

Fig. 4 Sample images of a subject from the AR face dataset. The first row represents the images from session 1 and the images from session 2 are shown in the second row

Fig. 5 Sample images of a subject from PubFig83 face dataset

4.2 Experimental setup

A three-layer network {L-M-N}(C) is used where the first layer has L = Q-1 inputs, the hidden layer has M $\mathbb{C}$HONs, the output layer consists of N = Ω summation aggregation neurons and C is the number of clusters which is equivalent to the number of associated networks. The inputs, weights, and biases in the network are all complex-valued. The assumptions regarding weights and biases are as follows: w_{lm} is the weight from l^{th} neuron to m^{th} neuron. $Z = \{z_1, z_2, \ldots, z_L\}$ represents the input vector, $W^s{}_m = \{w^s{}_{1m}, w^s{}_{2m}, \ldots, w^s{}_{Lm}\}$ be the weights from inputs to summation part of m^{th} $\mathbb{C}$HON and $W^{rb}{}_m = \{w^{rb}{}_{1m}, w^{rb}{}_{2m}, \ldots, w^{rb}{}_{Lm}\}$ be the weights provided to the radial basis part of m^{th} $\mathbb{C}$HON. $W_0 = \{w_{01}, w_{02}, \ldots, w_{0M}\}$ be the bias weights and zm_0 be the bias for M $\mathbb{C}$HONs in the hidden layer. $W_n = \{w_{1n}, w_{2n}, \ldots, w_{Mn}\}$ represents the weights of hidden neurons to n^{th} output neuron, $B_0 = \{b_{01}, b_{02}, \ldots, b_{0N}\}$ be the biases and zn_0 be the bias for N complex summation aggregation neurons in the output layer. Table 1 summarizes the setting of hyperparameters.

4.3 Quantitative analysis

We have conducted the performance evaluation of our model on a different combination of learning algorithms and hidden neurons: Real summation aggregation neurons with Real Backpropagation ($\mathbb{R}$SAN with $\mathbb{R}$BP), Real Higher Order Neurons with Real Backpropagation ($\mathbb{R}$HON with $\mathbb{R}$BP), Real summation aggregation neurons with Real Resilient Propagation ($\mathbb{R}$SAN with $\mathbb{R}$RPROP), Real Higher Order Neurons with Real Resilient Propagation ($\mathbb{R}$HON with $\mathbb{R}$RPROP), Complex summation aggregation neurons with Complex Back Propagation ($\mathbb{C}$SAN with $\mathbb{C}$BP), Complex Higher Order Neurons

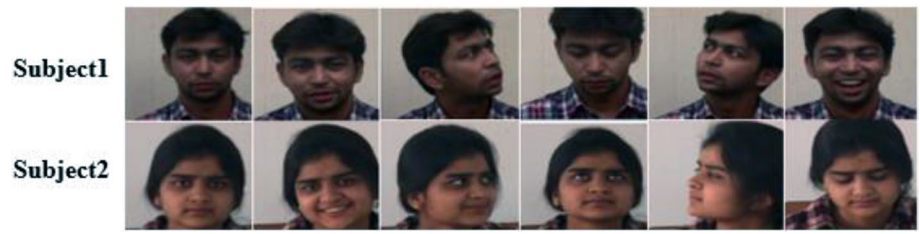

Fig. 6 Sample images from the Indian face dataset. The first row represents the variations of images for subject 1 while the second row represents the images for subject 2

Table 1 Hyperparameters Setting

Hyperparameters	Value
Fuzzifier	4
Generalization parameter	4
Learning rate	0.0015
$\mathbb{C}$RPROP learning initial step size	0.1
$\mathbb{C}$RPROP learning increasing factor	1.1
$\mathbb{C}$RPROP learning decreasing factor	1

with Complex Backpropagation ($\mathbb{C}$HON with $\mathbb{C}$BP), Complex summation aggregation neurons with Complex Resilient Propagation ($\mathbb{C}$SAN with $\mathbb{C}$RPROP), Complex Higher Order Neurons with Complex Resilient Propagation ($\mathbb{C}$HON with $\mathbb{C}$RPROP). The proposed model has been evaluated both on Sigmoid and Tanh activation functions [42]. For each dataset, the projected model is trained on the average training patterns and evaluated on test patterns. Tables 2, 3, and 4 represented the results for AR faces, PubFig83 faces, and Indian faces respectively where we have observed the following consequences: First, a classifier based on the $\mathbb{R}$HON and $\mathbb{C}$HON offers improved prediction precision in a considerably smaller number of training cycles as compared to $\mathbb{R}$SAN and $\mathbb{C}$SAN respectively for the same learning algorithm. Second, the accuracy precision of Tanh activation is superior that that of the Sigmoid function. Third, with a significantly fewer number of higher-order hidden neurons than conventional hidden neurons, the model achieved enhanced precision. While conducting the experiments, it has been observed that the number of hidden neurons, clusters, and preset members boost the performance up to some level, afterward, no additional improvement is noticed.

In Tables 2, 3, and 4, the values of a number of hidden neurons, clusters, and preset members are corresponding to the best-obtained results. The results depicted the superiority of higher-order neuron-based classifiers over their conventional neuron counterparts both in real and complex domain. We can observe that the accuracy attained for ($\mathbb{C}$HON,$\mathbb{C}$RPROP) variation is approximately 6% higher than that of ($\mathbb{R}$SAN, $\mathbb{R}$BP) variation of the classifier.

Table 2 Accuracy of the proposed model for 12 clusters and 16 preset members on the AR face dataset with Sigmoid and Tanh activation functions

(Hidden Neurons, Learning Algorithm)	Number of Hidden neurons	Learning Cycles	Accuracy with Sigmoid Activation Function	Accuracy with Tanh Activation Function
($\mathbb{R}$SAN, $\mathbb{R}$BP)	14	41,000	92.00%	92.70%
($\mathbb{R}$SAN, $\mathbb{R}$RPROP)	14	25,000	94.20%	94.80%
($\mathbb{R}$HON, $\mathbb{R}$BP)	6	30,000	93.80%	94.50%
($\mathbb{R}$HON, $\mathbb{R}$RPROP)	6	20,000	94.70%	95.00%
($\mathbb{C}$SAN, $\mathbb{C}$BP)	14	15,000	95.00%	95.20%
($\mathbb{C}$SAN, $\mathbb{C}$RPROP)	14	8500	96.80%	97.00%
($\mathbb{C}$HON, $\mathbb{C}$BP)	6	12,000	95.80%	96.20%
($\mathbb{C}$HON, $\mathbb{C}$RPROP)	**6**	**8000**	**97.40%**	**98.20%**

Boldface values represent the best results

Table 3 Accuracy of the proposed model for 12 clusters and 18 preset members on PubFig83 face dataset with Sigmoid and Tanh activation functions

(Hidden Neurons, Learning Algorithm)	Number of Hidden neurons	Learning Cycles	Accuracy with Sigmoid Activation Function	Accuracy with Tanh Activation Function
($\mathbb{R}$SAN, $\mathbb{R}$BP)	18	45,000	90.60%	91.40%
($\mathbb{R}$SAN, $\mathbb{R}$RPROP)	18	29,000	91.80%	92.10%
($\mathbb{R}$HON, $\mathbb{R}$BP)	9	35,000	92.40%	92.80%
($\mathbb{R}$HON, $\mathbb{R}$RPROP)	9	23,000	93.10%	93.30%
($\mathbb{C}$SAN, $\mathbb{C}$BP)	18	19,000	94.20%	94.80%
($\mathbb{C}$SAN, $\mathbb{C}$RPROP)	18	12,000	95.90%	96.60%
($\mathbb{C}$HON, $\mathbb{C}$BP)	9	17,000	95.00%	95.20%
($\mathbb{C}$HON, $\mathbb{C}$RPROP)	**9**	**9000**	**96.70%**	**97.85%**

Boldface values represent the best results

Table 5 presents the FAR and FRR values at different error thresholds for AR, PubFig83, and Indian face datasets. Figure 7a, b, and c shows the performance of our model on AR faces, PubFig83 faces and Indian faces grounded on FAR (false acceptance rate), and FRR (false rejection rate) [61]. The lower the values of FAR and FRR, the higher the efficacy of the system. The FAR and FRR are inversely proportional. The FAR-FRR graph is plotted for different error thresholds which gives an Equal Error Rate (EER) [53] at the point of intersection. EER is a metric to evaluate a biometric-based identification system. Our proposed framework gives the EER of 1.8%, 2.4%, and 1.2% for the AR face dataset, PubFig83 dataset, and Indian face dataset respectively. Figure 7d, e, and f show the ROC curves [61] where FRR is plotted at different FAR values for AR faces, PubFig83 faces, and Indian faces respectively. Figures 8, 9, and 10 portray the results with Sigmoid and Tanh activation functions for AR faces, PubFig83 faces and Indian faces respectively. The depicted results show the supremacy of the Tanh function over the Sigmoid function.

Table 4 Accuracy of the proposed model for 12 clusters and 12 preset members on the Indian face dataset with Sigmoid and Tanh activation functions

(Hidden Neurons, Learning Algorithm)	Number of Hidden neurons	Learning Cycles	Accuracy with Sigmoid Activation Function	Accuracy with Tanh Activation Function
($\mathbb{R}$SAN, $\mathbb{R}$BP)	15	40,000	92.00%	93.50%
($\mathbb{R}$SAN, $\mathbb{R}$RPROP)	15	27,000	94.10%	95.80%
($\mathbb{R}$HON, $\mathbb{R}$BP)	7	33,000	93.50%	95.10%
($\mathbb{R}$HON, $\mathbb{R}$RPROP)	7	21,000	95.00%	96.50%
($\mathbb{C}$SAN, $\mathbb{C}$BP)	15	18,500	95.40%	96.80%
($\mathbb{C}$SAN, $\mathbb{C}$RPROP)	15	10,000	96.70%	98.20%
($\mathbb{C}$HON, $\mathbb{C}$BP)	7	13,000	95.90%	97.40%
($\mathbb{C}$HON, $\mathbb{C}$RPROP)	**7**	**8000**	**97.80%**	**99.40%**

Boldface values represent the best results

Table 5 FAR and FRR values at different thresholds for AR, Pubfig83, and Indian face datasets

Error Threshold	AR		Pubfig83		Indian	
	FAR (%)	FRR (%)	FAR (%)	FRR (%)	FAR (%)	FRR (%)
1×10^{-3}	0.2	5.2	0.8	4.3	0.3	4.2
2×10^{-3}	0.6	3.0	1	3.8	0.6	3.5
3×10^{-3}	0.9	2.7	1.6	3.3	0.7	2.6
4×10^{-3}	1.2	2.3	2.5	2.4	0.9	2.3
5×10^{-3}	1.9	1.8	3.1	1.8	1	1.7
6×10^{-3}	2.3	1.3	4.8	1.0	1.2	1.2
7×10^{-3}	2.6	0.4	8.6	0.6	1.8	0.8
8×10^{-3}	3.8	0.2	9.3	0.4	2	0.3
1×10^{-2}	9.3	0.1	11.2	0.2	4.4	0.1
2×10^{-2}	11.5	0	18.3	0	5.7	0
3×10^{-2}	14.2	0	20.4	0	7.3	0

4.4 Ablation study

Our proposed recognizer is an integration of unsupervised and supervised frameworks. Let T be the training set, Eigenface Fisherface (EF) is an algorithm for feature extraction, complex fuzzy-c-means ($\mathbb{C}$FCM), and complex evolutionary computing ($\mathbb{C}$EC) constitutes complex unsupervised framework, complex neurocomputing ($\mathbb{C}$NN) referred to as a complex supervised framework. Different variants of the proposed model can be explained as follows:

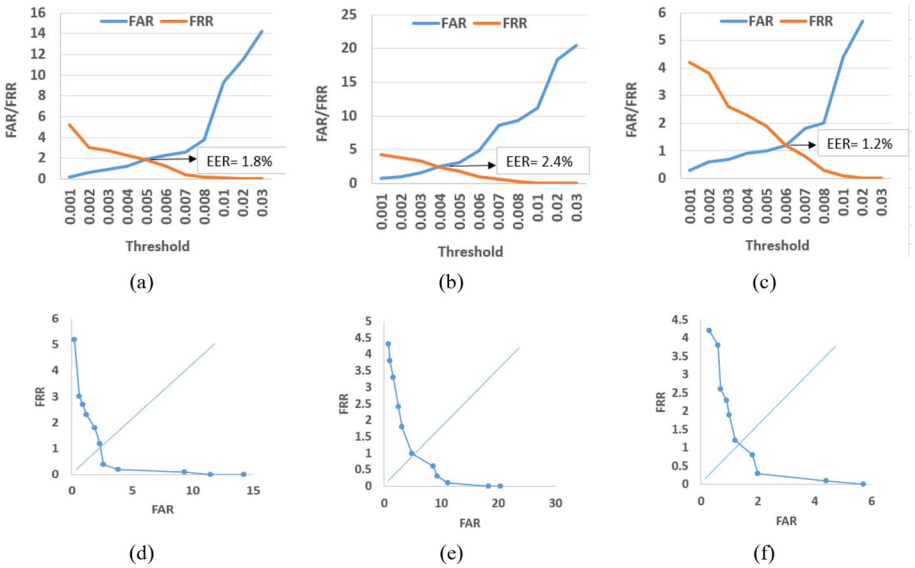

Fig. 7 First row shows FAR-FRR graphs which are plotted at different error thresholds. EER is obtained at the point where the graphs of FAR and FRR intersect (**a**) AR face dataset (**b**) PubFig83 dataset (**c**) Indian Face dataset. The second row shows the ROC curves where FRR is plotted at different FAR values (**d**) AR face dataset (**e**) PubFig83 dataset (**f**) Indian Face dataset

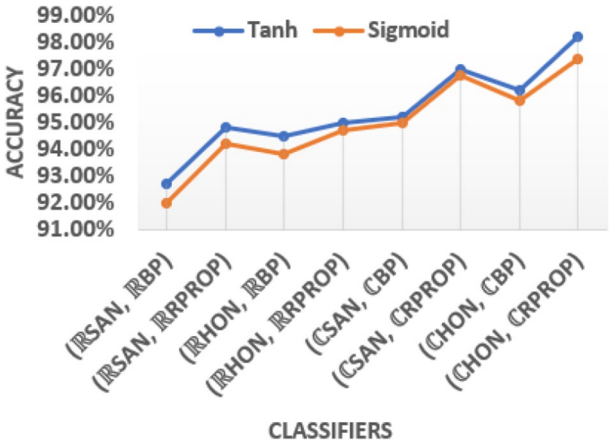

Fig. 8 Accuracy of different variations of hidden neuron and learning algorithm for AR face dataset

(1) **T + EF + ℂFCM**: In this variant, after feature extraction, we only considered complex fuzzy-c-means clustering
(2) **T + EF + ℂFCM + ℂEC**: In this variant, we used complex fuzzy-c-means supplemented with complex evolutionary computing.
(3) **T + EF + ℂNN:** In this variant, we used only complex neurocomputing.
(4) **T + EF + ℂFCM + ℂEC + ℂNN**: This is the complete version of the proposed model where we incorporated a complex unsupervised framework (ℂFCM + ℂEC) with a complex supervised framework (ℂNN).

Tables 6, 7, and 8 represent the ablation tests for the AR face dataset, PubFig83 face dataset, and Indian face dataset respectively. The ablations study shows that the accuracy only with either unsupervised or supervised frameworks is significantly less than that of unification of both frameworks. Figure 11 represents the results of the ablation study for AR faces, PubFig83 faces, and Indian faces. There is a gain of 13% to 15% in accuracy for the complete version of the model when compared to the initial version which can be easily witnessed in Fig. 12.

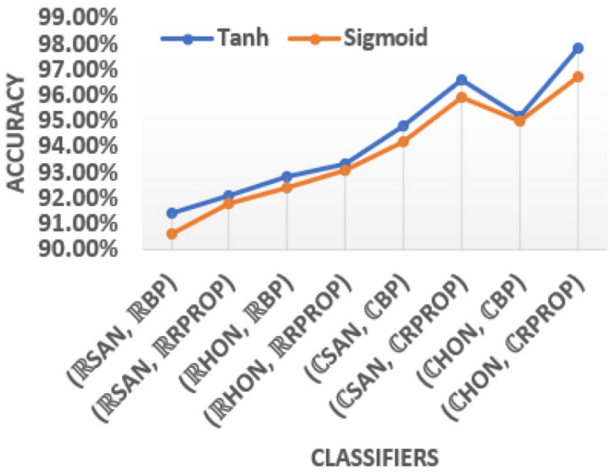

Fig. 9 Accuracy of different variations of hidden neuron and learning algorithm for PubFig83 face dataset

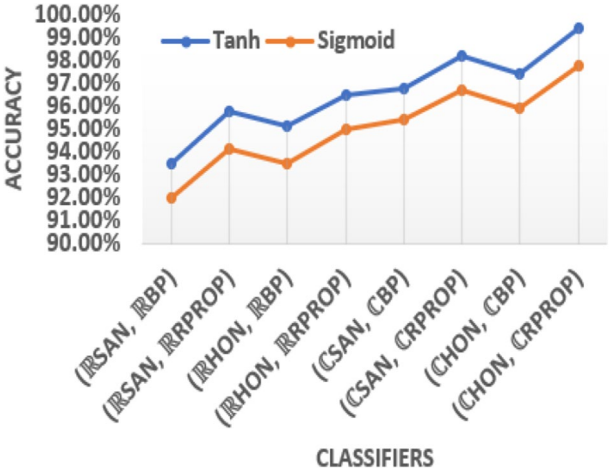

Fig. 10 Accuracy of different variations of hidden neuron and learning algorithm for Indian face dataset

Table 6 Ablation tests for the proposed model on AR face dataset

Variant	Accuracy
T + EF + $\mathbb{C}$FCM	82.13%
T + EF + $\mathbb{C}$FCM + $\mathbb{C}$EC	90.25%
T + EF + $\mathbb{C}$NN	94.82%
T + EF + $\mathbb{C}$FCM + $\mathbb{C}$EC + $\mathbb{C}$NN	**98.20%**

Boldface highlights highest accuracy values

Table 7 Ablation tests for the proposed model on PubFig83 face dataset

Variant	Accuracy
T + EF + $\mathbb{C}$FCM	80.62%
T + EF + $\mathbb{C}$FCM + $\mathbb{C}$EC	89.80%
T + EF + $\mathbb{C}$NN	93.00%
T + EF + $\mathbb{C}$FCM + $\mathbb{C}$EC + $\mathbb{C}$NN	**97.85%**

Boldface highlights highest accuracy values

Table 8 Ablation tests for the proposed model on Indian face dataset

Variant	Accuracy
T + EF + $\mathbb{C}$FCM	85.76%
T + EF + $\mathbb{C}$FCM + $\mathbb{C}$EC	91.62%
T + EF + $\mathbb{C}$NN	95.12%
T + EF + $\mathbb{C}$FCM + $\mathbb{C}$EC + $\mathbb{C}$NN	**99.40%**

Boldface highlights highest accuracy values

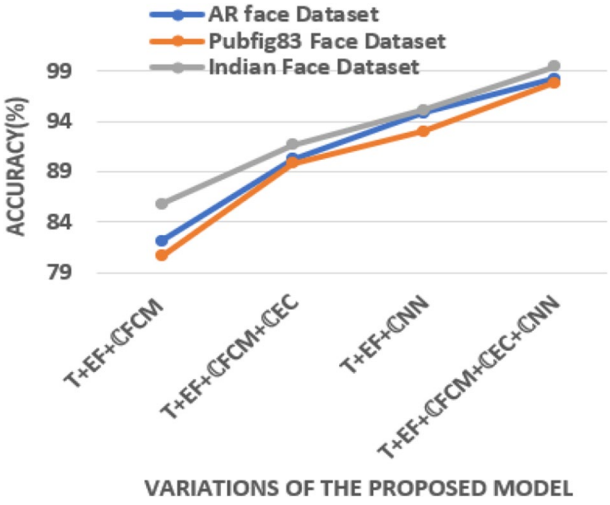

Fig. 11 Ablation Study for AR face dataset, PubFig83 dataset, and Indian Face dataset

4.5 Comparison with state-of-the-arts

This section presents the comparison of our model with existing methods. 5-fold cross-validation is applied to each dataset and the consequences are averaged to evaluate the efficacy of the proposed model. In Table 9 we have compared our results with recent recognizers on AR dataset. We trained our model on average training patterns and evaluated on test patterns. The proposed model attains 2.01% higher accuracy than the best

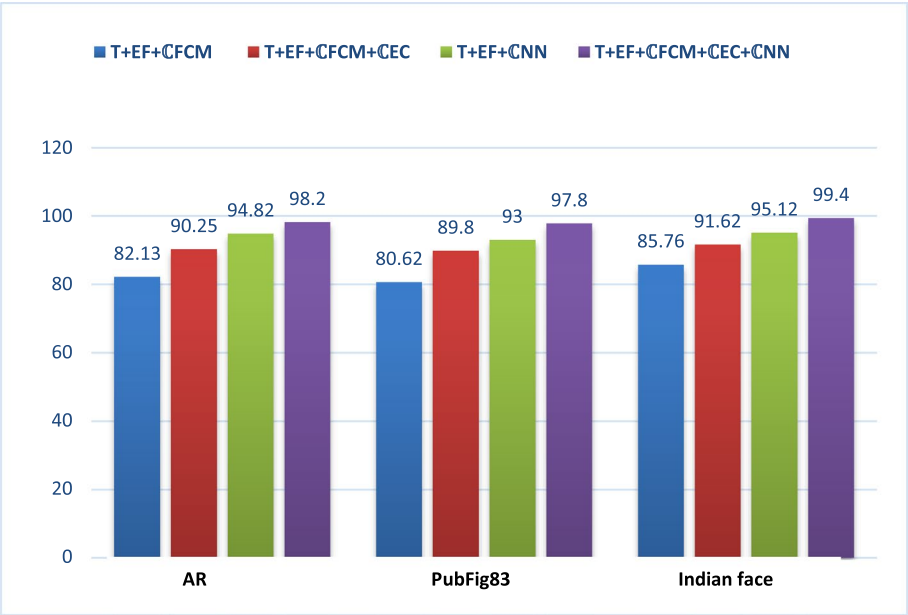

Fig. 12 Ablation results for AR, PubFig83, and Indian Face Datasets

Table 9 Accuracy of the proposed model and state-of-the-art methods for the AR face dataset

Model	Features/Methods/ Techniques Used	Accuracy
Fontaine et al. [27]	Robust Sparse Coding algorithm	95.00%
Aslan et al. [5]	K-means clustering and HOG, Hand crafted, autoencoder, and deep feature learning techniques	95.04%
Agarwal & Bhanot, [2]	evolutionary firefly algorithm, radial basis function neural network	93.15%
Faraji & Qi [24]	log function, MR filter,multi-scale Gradientface method,	91.91%
Chen et al. [10]	discriminative learning, structured dictionary pair learning	96.19%
Zhang et al. [71]	Sparsity with Nonconvex Regression	91.00%
Chen et al. [9]	Deep-Layer Cascaded Representation	96.10%
Ours (T + EF + $\mathbb{C}$FCM)	Complex Fuzzy-c-means clustering	82.13%
Ours (T + EF + $\mathbb{C}$FCM + $\mathbb{C}$EC)	Complex FCM and Evolutionary computation	90.25%
Ours (T + EF + $\mathbb{C}$NN)	Complex NN	94.82%
Ours (T + EF + $\mathbb{C}$FCM + $\mathbb{C}$EC + $\mathbb{C}$NN)	**Complex FCM with Evolutionary computation and Complex NN**	**98.20%**

Boldface highlights highest accuracy values

Table 10 Accuracy of the proposed model and state-of-the-art methods for PubFig83 face dataset

Model	Features/Methods/ Techniques Used	Accuracy
Chen et al. [8]	Supervised and unsupervised learning, Deep Autoencoder and Deep learning	90.14%
Chiachia et al. [11]	person-specific partial least squares method	92.28%
Aslan et al. [5]	K-means clustering and HOG, Hand crafted, autoencoder, and deep feature learning techniques	95.85%
Ergul [19]	RBF kernel-based one-vs-all SVM, Supervised attributes, and unsupervised attributes	84.05%
Görgel & Simsek [30]	deep neural network technology, sparse autoencoders, multi-class SVM, and Softmax classifier.	95.20%
Chen et al. [10]	discriminative learning, structured dictionary pair learning	62.10%
Chen et al. [9]	Deep-Layer Cascaded Representation	64.30%
Ours (T + EF + $\mathbb{C}$FCM)	Complex Fuzzy-c-means clustering	80.62%
Ours (T + EF + $\mathbb{C}$FCM + $\mathbb{C}$EC)	Complex FCM and Evolutionary computation	89.80%
Ours (T + EF + $\mathbb{C}$NN)	Complex NN	93.00%
Ours (T + EF + $\mathbb{C}$FCM + $\mathbb{C}$EC + $\mathbb{C}$NN)	**Complex FCM with Evolutionary computation and Complex NN**	**97.85%**

Boldface highlights highest accuracy values

Table 11 Accuracy of the proposed model and state-of-the-art methods for the Indian face dataset

Model	Features/Methods/ Techniques Used	Accuracy
Arivazhagan et al. [4]	Local Directional Number Pattern, Soft Computing Technique, and ANFIS Classifier	90.47%
Tripathi [64]	CICA, CPCA and OCON Classifier	97.20%
Choudhury [12]	PCA, HOG, Blob Classifier	94.00%
Fawwad Hussain et al. [25]	SC features	66.00%
Fawwad Hussain et al. [25]	PHOG features	70.00%
Fawwad Hussain et al. [25]	Gist features	70.00%
Choudhury & Rabbani [13]	PCA, canny edge detector, and SURF algorithm	98.99%
Sardar et al. [56]	LDA, K-means, and SVM	72.38%
Ours (T + EF + $\mathbb{C}$FCM)	Complex Fuzzy-c-means clustering	85.76%
Ours (T + EF + $\mathbb{C}$FCM + $\mathbb{C}$EC)	Complex FCM and Evolutionary computation	91.62%
Ours (T + EF + $\mathbb{C}$NN)	Complex NN	95.12%
Ours (T + EF + $\mathbb{C}$FCM + $\mathbb{C}$EC + $\mathbb{C}$NN)	**Complex FCM with Evolutionary computation and Complex NN**	**99.40%**

Boldface highlights highest accuracy values

result of the previous recognizer [10] on the AR dataset. Table 10 demonstrates the gain of approx. 2% in resulting accuracy over the best previous results obtained by model [5] on the PubFig83 dataset. Table 11 demonstrates the results obtained with the proposed model on the Indian face dataset where the gain of 0.41% is observed in accuracy over the best state-of-the results. The obtained accuracies for all considered datasets show the supremacy of the final version of the proposed model **(T + EF + ℂFCM + ℂEC + ℂNN)** over other versions of the proposed model as well as state-of-the-art methods.

5 Conclusions and future scope

In this work, we proposed a face recognition model which is an integration of complex unsupervised and complex supervised frameworks. The eigenface with fisherface method is used to extract the desired features from input images. For unconstrained faces, robust and efficient fuzzy clustering is employed in unsupervised module. Evolutionary computation surpasses the stochastic nature of fuzzy clustering by enabling a self-adaptive search for optimal solutions which results in a cluster dispersal matrix. This outcome of the unsupervised module is used for two purposes; (1) to decide the structure of the neural network (2) to train the networks. The network is built up on the ℂHON where error is optimized through ℂRPROP learning. The novel unification of complex unsupervised framework and complex domain neurocomputing illustrated better generalization than existing methods. To prevent the system from surplus computational complexity, the ℂHON is used only in the hidden layer of the network. Its use in the output layer can be considered as future work that will indisputably expand the performance of the model.

Declarations

Conflict of interest The authors declare that they have no conflict of interest.

References

1. Abuzneid MA, Mahmood A (2018) Enhanced human face recognition using LBPH descriptor, multi-KNN, and back-propagation neural network. IEEE Access 6:20641–20651
2. Agarwal V, Bhanot S (2018) Radial basis function neural network-based face recognition using firefly algorithm. Neural Comput & Applic 30(8):2643–2660
3. Anggo M, Arapu L (2018) Face recognition using fisherface method. J Phys Conf Ser 1028(1):012119 IOP Publishing
4. Arivazhagan S, Priyadharshini RA, Sowmiya S (2014) Face recognition based on local directional number pattern and ANFIS classifier. In: Int. Conference on Advanced Communication Control and Computing Technologies (ICACCCT), pp 1627–1631
5. Aslan MS, Hailat Z, Alafif TK, Chen XW (2017) Multi-channel multi-model feature learning for face recognition. Elsevier, Pattern Recognit Lett 85:79–83
6. Belhumeur PN, Hespanha JP, Kriegman DJ (1997) Eigenfaces vs. fisherfaces: Recognition using class specific linear projection. IEEE Trans Pattern Anal Mach Intell 19(7):711–720
7. Çevik HH, Acar YE, Çunkaş M (2018) Day ahead wind power forecasting using complex valued neural network. In: 2018 International Conference on Smart Energy Systems and Technologies (SEST). IEEE. pp 1–6
8. Chen XW, Aslan M, Zhang K, Huang T (2015) Learning multi-channel deep feature representations for face recognition. In: Feature Extraction: Modern Questions and Challenges, pp 60–71

9. Chen Z, Wu XJ, Xu T, Kittler J (2021) Learning alternating deep-layer cascaded representation. IEEE Signal Processing Letters 28:1520–1524
10. Chen Z, Wu XJ, Xu T, Kittler J (2022) Discriminative dictionary pair learning with scale-constrained structured representation for image classification. IEEE Trans Neural Netw Learn Syst PP:1–15
11. Chiachia G, Falcao AX, Pinto N, Rocha A, Cox D (2014) Learning person-specific representations from faces in the wild. IEEE Trans Inf Forensics Secur 9(12):2089–2099
12. Choudhury ZH (2019) Biometrics passport authentication using facial Marks.
13. Choudhury ZH, Rabbani MMA (2021) Facial blemishes detection and encryption with secure force algorithm into HCC2D code for biometric-passport. Inf Secur J: A Global Perspective 30(6):342–358
14. Cui Y, Yi Z, Duan J, Shi D, Wang Z (2019) A Rprop-neural-network-based PV maximum power point tracking algorithm with short-circuit current limitation. In: 2019 IEEE Power & Energy Society Innovative Smart Grid Technologies Conference (ISGT). IEEE. pp 1–5
15. Dadi HS, Pillutla GKM, Makkena ML (2018) Face recognition and human tracking using GMM, HOG and SVM in surveillance videos. Ann Data Sci 5(2):157–179
16. Dash R (2018) Performance analysis of a higher order neural network with an improved shuffled frog leaping algorithm for currency exchange rate prediction. Appl Soft Comput 67:215–231
17. Egrioglu E, Yolcu U, Bas E (2019) Intuitionistic high-order fuzzy time series forecasting method based on pi-sigma artificial neural networks trained by artificial bee colony. Granular Computing 4(4):639–654
18. Er MJ, Wu S, Lu J, Toh HL (2002) Face recognition with radial basis function (RBF) neural networks. IEEE Trans Neural Netw 13(3):697–710
19. Ergul E (2017) Relative attribute based incremental learning for image recognition. CAAI Trans Intell Technol 2(1):1–11
20. Everitt BS, Dunn G (2001) Applied multivariate data analysis, vol 2. Arnold, London
21. Fan F, Wang G (2020) Fuzzy logic interpretation of quadratic networks. Neurocomputing 374:10–21
22. Fan F, Shan H, Kalra MK, Singh R, Qian G, Getzin M, … Wang G (2019) Quadratic autoencoder (Q-AE) for low-dose CT denoising. IEEE Trans Med Imaging 39(6):2035–2050
23. Fan F, Xiong J, Wang G (2020) Universal approximation with quadratic deep networks. Neural Netw 124:383–392
24. Faraji MR, Qi X (2018) Face recognition under varying illuminations with multi-scale gradient maximum response. Neurocomputing 308:87–100
25. Fawwad Hussain M, Wang H, Santosh KC (2018) Gray level face recognition using spatial features. In: International Conference on Recent Trends in Image Processing and Pattern Recognition. Springer, Singapore, pp 216–229
26. Fisher RA (1936) The use of multiple measurements in taxonomic problems. Ann Hum Genet 7(2):179–188
27. Fontaine X, Achanta R, Süsstrunk S (2017) Face recognition in real-world images. In: IEEE Int. Conference on Acoustics, Speech and Signal Processing (ICASSP), pp. 1482–1486
28. Gao J, Deng B, Qin Y, Wang H, Li X (2018) Enhanced radar imaging using a complex-valued convolutional neural network. IEEE Geosci Remote Sens Lett 16(1):35–39
29. Gautam A, Bhateja V, Tiwari A, Satapathy SC (2018) An improved mammogram classification approach using back propagation neural network. In: Data Engineering and Intelligent Computing. Springer, Singapore, pp 369–376
30. Görgel P, Simsek A (2019) Face recognition via deep stacked denoising sparse autoencoders (DSDSA). Appl Math Comput 355:325–342
31. Gupta M (2021) An efficacious method for face recognition using DCT and neural network. In: Sustainable communication networks and application. Springer, Singapore, pp 671–683
32. Hair JF, Black WC, Babin BJ, Anderson RE, Tatham RL (1998) Multivariate data analysis, Upper Saddle River: Prentice hall, 5(3): 207–219
33. Hataya R, Zdenek J, Yoshizoe K, Nakayama H (2020) Faster autoaugment: Learning augmentation strategies using backpropagation. In: European Conference on Computer Vision. Springer, Cham, pp 1–16
34. Hathaliya JJ, Tanwar S, Evans R (2020) Securing electronic healthcare records: A mobile-based biometric authentication approach. J Inf Secur Appl 53:102528
35. He X, Yan S, Hu Y, Niyogi P, Zhang HJ (2005) Face recognition using laplacianfaces. IEEE Trans Pattern Anal Mach Intell 27(3):328–340
36. Hermanto RPS, Nugroho A (2018) Waiting-time estimation in bank customer queues using RPROP neural networks. Procedia Comput Sci 135:35–42
37. Jain V (2002) The Indian face database. http://vis-www.cs.Umass.edu/vidit/IndianFaceDatabase. Accessed 10 Jan 2022

38. Javed Mehedi Shamrat FM, Ghosh P, Tasnim Z, Khan AA, Uddin M, Chowdhury TR (2022) Human face recognition using eigenface, SURF method. In: Pervasive Computing and Social Networking. Springer, Singapore, pp 73–88
39. Jia L, Yang B, Zhang W (2018) Research on stock forecasting based on GPU and complex-valued neural network. In: International Conference on Intelligent Computing. Springer, Cham, pp 120–128
40. Johansson M (1999) The hilbert transform. Mathematics Master's Thesis. Växjö University, Suecia. Disponible en internet: http://w3.msi.vxu.se/exarb/mj_ex.pdf, consultadoel, 9. Accessed 18 Jan 2022
41. Kakkad V, Patel M, Shah M (2019) Biometric authentication and image encryption for image security in cloud framework. Multiscale Multidiscip Model Exp Des 2(4):233–248
42. Karlik B, Olgac AV (2011) Performance analysis of various activation functions in generalized MLP architectures of neural networks. Int J Artif Intell Exp Syst 1(4):111–122
43. Katoch S, Chauhan SS, Kumar V (2021) A review on genetic algorithm: past, present, and future. Multimed Tools Appl 80(5):8091–8126
44. Kumaar S, Vishwanath RM, Omkar SN, Majeedi A, Dogra A (2018) Disguised facial recognition using neural networks. In: 2018 IEEE 3rd International Conference on Signal and Image Processing (ICSIP). IEEE. pp 28–32
45. Li L, Wang Z, Li Y, Shen H, Lu J (2018) Hopf bifurcation analysis of a complex-valued neural network model with discrete and distributed delays. Appl Math Comput 330:152–169
46. Liu C, Wechsler H (2002) Gabor feature based classification using the enhanced fisher linear discriminant model for face recognition. IEEE Trans Image Process 11(4):467–476
47. Lukas S, Mitra AR, Desanti RI, Krisnadi D (2016) Student attendance system in classroom using face recognition technique. In: IEEE Int. Conference on Information and Communication Technology Convergence (ICTC), pp 1032–1035
48. Mantoro T, Ayu MA (2018) Multi-faces recognition process using Haar cascades and eigenface methods. In: 2018 6th International Conference on Multimedia Computing and Systems (ICMCS). IEEE. pp 1–5
49. Martinez AM (1998) The AR face database. CVC Technical Report24
50. Nemati S, Rohani R, Basiri ME, Abdar M, Yen NY, Makarenkov V (2019) A hybrid latent space data fusion method for multimodal emotion recognition. IEEE Access 7:172948–172964
51. Oyama K, Hirose A (2018) Performance of entire-spectrum-processing complex-valued neural-network filter to generate digital elevation model in interferometric radar. In: 2018 International Joint Conference on Neural Networks (IJCNN). IEEE. pp 1–7
52. Pinto N, Stone Z, Zickler T, Cox D (2011) Scaling up biologically-inspired computer vision: A case study in unconstrained face recognition on facebook. In: IEEE Computer Society Conference on Computer Vision and Pattern Recognition Workshops (CVPRW), pp 35–42
53. Rajasekar V, Predić B, Saracevic M, Elhoseny M, Karabasevic D, Stanujkic D, Jayapaul P (2022) Enhanced multimodal biometric recognition approach for smart cities based on an optimized fuzzy genetic algorithm. Sci Rep 12(1):1–11
54. Rejeesh MR (2019) Interest point based face recognition using adaptive neuro fuzzy inference system. Multimed Tools Appl 78(16):22691–22710
55. Roh SB, Oh SK, Yoon JH, Seo K (2019) Design of face recognition system based on fuzzy transform and radial basis function neural networks. Soft Comput 23(13):4969–4985
56. Sardar A, Umer S, Rout RK, Wang SH, Tanveer M (2023) A secure face recognition for IoT-enabled healthcare system. ACM Trans Sensor Netw 19(3):1–23
57. Sasirekha K, Thangavel K (2019) Optimization of K-nearest neighbor using particle swarm optimization for face recognition. Neural Comput & Applic 31(11):7935–7944
58. Seha SNA, Hatzinakos D (2020) EEG-based human recognition using steady-state AEPs and subject-unique spatial filters. IEEE Trans Inf Forensics Secur 15:3901–3910
59. Sharma S, Bhatt M, Sharma P (2020) Face recognition system using machine learning algorithm. In: 2020 5th International Conference on Communication and Electronics Systems (ICCES). IEEE. pp 1162–1168
60. Shi B, Bai X, Yao C (2017) An end-to-end trainable neural network for image-based sequence recognition and its application to scene text recognition. IEEE Trans Pattern Anal Mach Intell 39(11):2298–2304
61. Srivastava S, Agarwal S (2011) Offline signature verification using grid based feature extraction. In: IEEE Int. Conference on Computer and Communication Technology (ICCCT), pp 185–190
62. Srivastava S, Tripathi B (2018) On the Deep Hybrid Computational Model for Face Recognition. Int J Intell Eng Syst 11(1):121–130
63. Tabachnick BG, Fidell LS (2007) Using multivariate statistics. Allyn and Bacon/Pearson Education

64. Tripathi BK (2017) On the complex domain deep machine learning for face recognition. Appl Intell 47(2):382–396
65. Tripathi BK, Kalra PK (2011) On efficient learning machine with root-power mean neuron in complex domain. IEEE Trans Neural Netw 22(5):727–738
66. Tuncer T, Dogan S, Akbal E (2019) Discrete complex fuzzy transform based face image recognition method. Int J Image Graph Signal Process (IJIGSP) 11(4):1–7
67. Venkatachalam K, Prabu P, Almutairi A, Abouhawwash M (2021) Secure biometric authentication with de-duplication on distributed cloud storage. PeerJ Computer Science 7:e569
68. Virtue P, Stella XY, Lustig M (2017) Better than real: complex-valued neural nets for MRI fingerprinting. In: 2017 IEEE international conference on image processing (ICIP). IEEE. pp 3953–3957
69. Welling M (2005) Fisher linear discriminant analysis. Department of Computer Science, University of Toronto, 3(1)
70. Xu Z, Xiong J, Yu F, Chen X (2020) Efficient Neural Network Implementation with Quadratic Neuron. arXiv preprint arXiv:2011.10813
71. Zhang C, Li H, Chen C, Qian Y, Zhou X (2020) Enhanced group sparse regularized nonconvex regression for face recognition. IEEE Trans Pattern Anal Mach Intell 44(5):2438–2452